Magnon Thermal Conductivity of Solid ^{3}He in the U2D2 Antiferromagnetic Phase

Y. P. Feng, P. Schiffer, J. Mihalisin,[a] and D. D. Osheroff
Department of Physics, Stanford University, Stanford, California 94305
(Received 17 April 1990; revised manuscript received 15 August 1990)

We report the first measurement of magnon thermal conductivity in monodomain single crystals of ^{3}He in the U2D2 antiferromagnetic phase. The magnon mean free path λ was found first to rise rapidly upon cooling below T_N and then more slowly at low temperatures, depending upon the sample. The temperature dependence is consistent with magnon umklapp scattering at high T, i.e., λ proportional to $T^{-2}\exp(\Delta/k_BT)$, with Δ/k_B determined to be 5.8($\pm$0.3) mK. The limiting low-temperature values of λ varied from 0.3 to 3 μm.

PACS numbers: 67.80.Gb, 75.30.Ds

The U2D2 nuclear antiferromagnetic phase of solid ^{3}He offers a unique opportunity to study magnon thermal transport. Previous measurements in electronic antiferromagnets have been troubled by significant phonon conduction and phonon-magnon scattering,[1-3] which are expected to be unimportant in the U2D2 phase. Since at submillikelvin temperatures few phonons are thermally excited, magnons are the only heat carriers and magnon scattering dictates thermal conduction. If the magnon mean free path is not limited by defects in the magnetic sublattice structure, magnon umklapp scattering will be responsible for finite thermal resistance. We have used the strong temperature dependence of the antiferromagnetic resonance in the U2D2 phase as a contactless thermometer, which not only has submicrokelvin resolution, but also allows a determination of the entire thermal distribution across a quasi-one-dimensional heat-carrying single crystal.

Single crystals of solid ^{3}He were nucleated and grown inside a cylindrical channel 1.2 cm long and 1 mm in diameter, within a crystal-growth cell constructed of Vespel[4] (SP21) as depicted in Fig. 1. A NMR coil was wound along the length of the channel. The cell was inserted into the bottom of a variable-volume compression device described previously,[5] which included a strain gauge for pressure measurement. The compression device was then mounted on a copper nuclear demagnetization apparatus,[5] capable of cooling samples of 0.35 mK with a warm-up rate of about 0.2 μK/h. A nucleation heater was placed at the bottom of the channel, electrically connected to a pulse generator via an isolation transformer inside the cell in order to break the thermal link to the outside. Stray heat leaks into our samples are estimated to have been only about 0.02 pW. Vespel's low thermal conductivity assured thermal isolation of the solid, which came into contact with the superfluid only at the upper open end of the growth channel. The antiferromagnetic resonance was measured using a conventional cw NMR spectrometer with a two-axis magnet, capable of generating a magnetic field homogeneous to 10 ppm over a cubic centimeter in space. A device was installed to turn the biaxial magnet, allowing us to rotate the field to any direction in space while maintaining a U2D2 crystal below 1 mK. The magnetic field decayed at a rate no greater than 6 parts in 10^8 per hour.

Crystals were grown directly from the superfluid B phase[6] in a strain-free environment, and were never subjected to strain levels beyond the 2-mbar change in hydrostatic melting presure associated with changes in temperature. The liquid was first precooled to 0.4 mK with a hydrostatic cell pressure about 100 mbar below the melting curve. The cell pressure was then raised to $\sim$1.2 mbar above the melting pressure and a 1-msec ac heat pulse of about 2 ergs was applied, initiating the solid growth. The cell pressure was maintained roughly 1 mbar above the melting pressure during growth. The amount of solid in the channel was calculated directly from the integral of the NMR signal, since the magnetic susceptibility $\chi_\perp$ of U2D2 solid ^{3}He is essentially temperature independent[7,8] (in the U2D2 phase, the sublat-

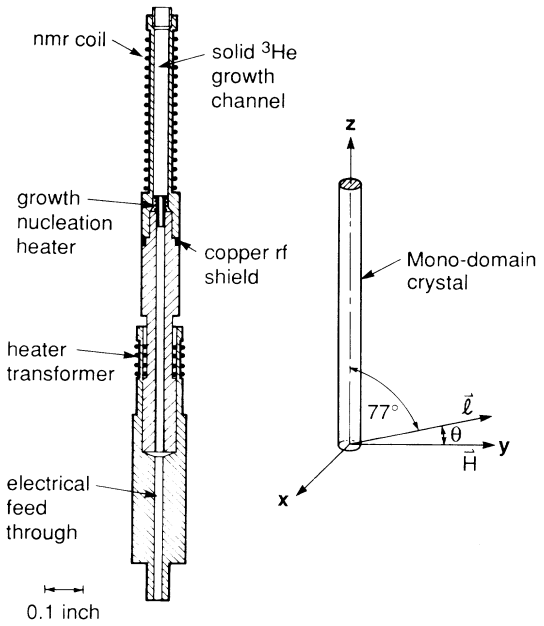

FIG. 1. Cross section of solid-^{3}He single-crystal growth cell. The domain orientation ($\boldsymbol{l}$) of a monodomain crystal is also shown with respect to the applied magnetic field ($\mathbf{H}$) and the heat flow along the crystal axis (z).

tice magnetization always adjusts itself to be perpendicular to the external magnetic field[9]).

The U2D2 magnetic structure in a bcc lattice consists of ferromagnetic planes of spins normal to one of the cube axes with successive planes having their spins oriented up, up, down, down.[9] We denote the domain orientation as the direction normal to these planes. We were able to grow effectively monodomain samples, even though there were always three domains in our crystals immediately after nucleation. Under the right conditions, as yet not understood, only the domain most nearly normal to the growth direction would continue to grow and fill the entire channel, so that the final volume of this dominant domain was typically 95% of the total. Our ability to achieve this preferential growth was strongly linked to the amount of nucleation heat used: A smaller heat input above a threshold improved the likelihood of obtaining a monodomain crystal, but slowed the growth process appreciably. We concluded that the solid was able to fill the channel effectively, since the integral of the NMR signal was reproducible to better than 1% for fully grown crystals. This implied that the crystals' cross sections were uniform to 2 μm.

Thermal relaxations of monodomain crystals were measured between 0.35 and 0.9 mK. A crystal was first brought into thermal equilibrium with the liquid, establishing a monotonic temperature distribution across its entire length. The liquid temperature was then raised abruptly through remagnetization. The solid relaxed toward a new equilibrium distribution, with heat passing through the open upper end from the liquid. The instantaneous NMR spectrum was then recorded at equal time intervals, as shown in Fig. 2(a), to monitor the evolution of the crystal's thermal distribution. The thermal boundary resistances between the superfluid and the solid ^{3}He and between the superfluid and the heat exchanger were sufficiently small that the temperature of the upper (warm) end of the crystal stayed essentially constant during the relaxation process. This is manifested by the constant position of the absorption edge at the low-frequency end of the spectrum. The time interval Δt was chosen to be much shorter than the relaxation time for the whole crystal, which ranged from several minutes at the lowest temperatures to a few tens of hours near the Néel temperature.

We deduced the thermal distribution by deconvoluting the NMR signal and utilizing the monotonic temperature dependence of the antiferromagnetic resonance frequency Ω, originally measured by Osheroff, Cross, and Fisher[9] (OCF). In order to deconvolute we made the following assumptions: the monodomain crystals were quasi one dimensional, the magnetic susceptibility of the U2D2 phase is temperature independent, and the temperature varied monotonically along the length of the crystal. Then, for any frequency ν on the NMR profile, all of the signal on the low-frequency side originated from the solid on the high-temperature side of a corresponding position z in the crystal. We calculated z by integrating the NMR signal from the highest frequency (corresponding to the cold end) to the frequency ν. The temperature $T(z)$ was then evaluated from ν using a polynominal fit to the data given by OCF,[9]

$$T/T_N = 2.536 - 1.647X + 0.734X^2 - 0.169X^3 + 1.91\times10^{-2}X^4 - 8.9\times10^{-4}X^5, \quad (1)$$

where $X = \Omega^2/(4\pi^2\times10^{11})$, $T_N = 0.932$ mK is the Néel temperature,[10] and Ω is calculated with

$$\Omega/2\pi = \{\nu^2(\nu^2 - \nu_L^2)/[\nu^2 - \nu_L^2(1-\cos^2\theta)]\}^{1/2},$$

where θ is the angle between the monodomain orientation and the magnetic field, and ν_L is the Larmor frequency. For our experiment we used $\nu_L = 2.1$ MHz.

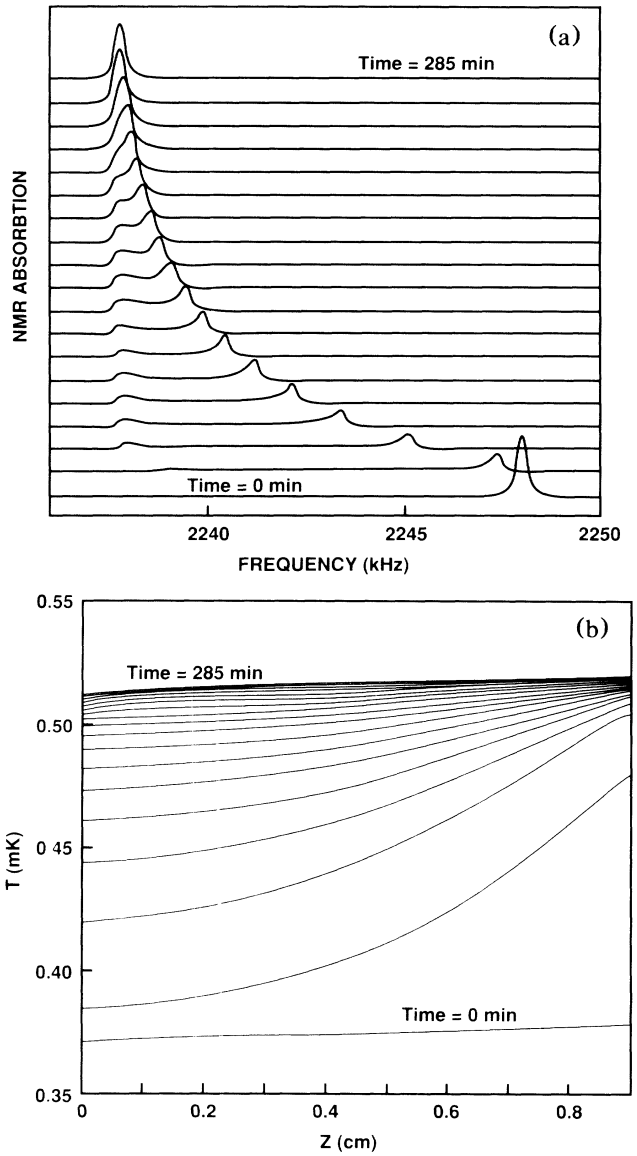

FIG. 2. (a) Instantaneous NMR spectra, and (b) thermal distributions for a monodomain crystal at equal time intervals during a thermal relaxation. Notice that the initial and the final states are nearly thermally equilibrated.

Thus we obtained temperature as a function of both time and position as shown in Fig. 2(b), where $T(z)$ is plotted at equally separated time intervals during a single relaxation for crystal D. The liquid-^{3}He NMR linewidth was about 30 Hz, and we typically measured a width of 250 Hz in the solid. From the variation of this linewidth with field orientation, we estimate that any possible mosaic spread of our single crystals had to be less than about 1 arc min over the entire 1-cm length of our samples. We were able to resolve the temperature to better than 1 μK since the resolution depended only on our ability to distinguish the shift of the NMR spectrum, which was measurable to 10 Hz. The small drift in ν_L due to field decay resulted in a negligible shift in the temperature scale of less than 1 μK over a two-week period.

The thermal conductivity κ was calculated using the expression $dQ/dt = -A\kappa dT/dz$, where A is the cross-sectional area, and we have assumed that heat flows only in the z direction. The determine dQ/dt at every point on the crystal, we integrated the heat content in the crystal below that point, and then took the difference in heat contents found for successive NMR spectra. To find the heat content, we have used the heat capacity $C = 2.0 \times 10^8 T^3$ J/cm^{3}K^4, combining earlier melting-pressure[11] and heat-capacity[12] measurements. We have also used finite-element analysis to model the relaxation of our crystals, and find excellent agreement with the results of the technique described above. Here κ should be attributed only to thermal conduction by acoustic magnons. Since the optical branches of magnons have energies roughly twice as high as those of the acoustic branch,[13] their contribution can be ignored below 1 mK. Phonon and acoustic-magnon coupling occurs only where their dispersion curves cross, with energy of 2 MHz (100 μK) in our experiment and wave vector $q \approx 0$, due to the vast difference between magnon and phonon velocities.[11,14] Thus the effects of phonon-magnon scattering and possible phonon emission due to this coupling are small based on phase-space considerations. Furthermore, because the Debye temperature of solid ^{3}He at melting pressure is about 17 K,[14] 4 orders of magnitude larger than the Néel temperature, thermal phonons are scarce and their direct contribution to thermal transport is negligible. Thermal conduction through possible needlelike liquid pockets near the wall is also judged insignificant, because such conduction would have given rise to a completely different temperature dependence than that seen experimentally, due to the exponentially dropping conductivity of the liquid in the limit where the mean free path is limited by boundary scattering. Values of the thermal conductivity determined in this manner are shown in Fig. 3 for two crystals, A and D, which we have studied extensively.

Assuming that the dispersion relation for acoustic magnons is analogous to that of phonons,[15] the language of phonon scattering can be applied in discussing magnon thermal conductivity.[16] The magnon mean free path λ is obtained using the simple expression from kinetic theory $\kappa = \frac{1}{3} C v \lambda$, where $V = 7.7$ cm/sec is the magnon velocity.[11,12] In Fig. 4 we show values of λ for crystals A and D. Plotted are values of $\ln(\lambda)$ vs $1/T$, with λ in μm and T in mK. By measuring the NMR spectra of all three domains from each crystal in two separate magnetic-field orientations, we were able to determine the orientations of the principal crystalline axes for these bcc structures to have been (85°, 96°), (34°, 358°), and (54°, 189°) for crystal A, and (75°, 319°), (36°, 209°), and (58°, 59°) for crystal D. Here the first angle is the polar angle relative to the heat-flow direction, the second is the azimuthal angle, and the dominant domain was oriented along the first axis listed for each crystal.

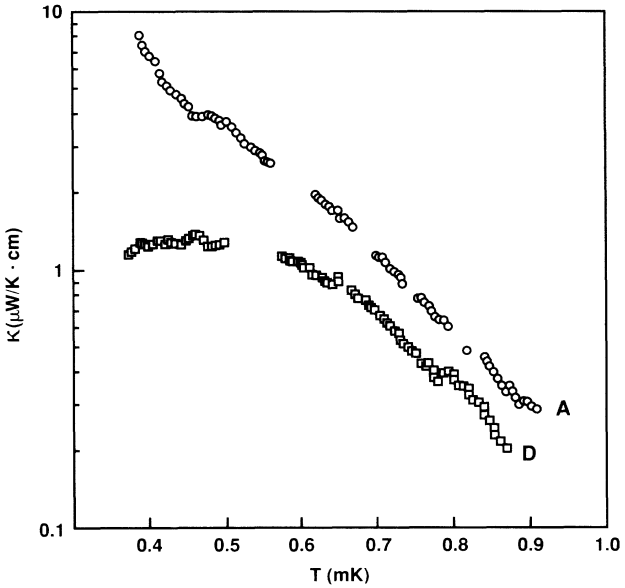

FIG. 3. Thermal conductivity κ of two monodomain single crystals (○, crystal A; □, crystal D) measured in the temperature range between 0.35 and 0.90 mK.

The solid lines in Fig. 4 represent fits to the data of the form

$$\frac{1}{\lambda} = \frac{T^2}{\lambda_0} \exp\left(-\frac{\Delta}{k_B T}\right) + \frac{T^a}{\lambda_1}. \quad (2)$$

Here the first term represents umklapp scattering, and the exponent of the temperature-dependent prefactor has been determined by Fisher to be 2.[17] The term λ_0 depends upon the density of states of magnons. The activation energy Δ is the energy of a zone-boundary magnon, and because of the exponential term, usually has a value near that of the lowest zone-boundary magnon with a momentum component along the heat-flow direction. The second term represents scattering of magnons off magnetic defects, and the temperature dependence is presumably determined by the density of states of the magnons and the dimensionality of the scattering sites. To best fit our data, we find that a must be 3 for crystal

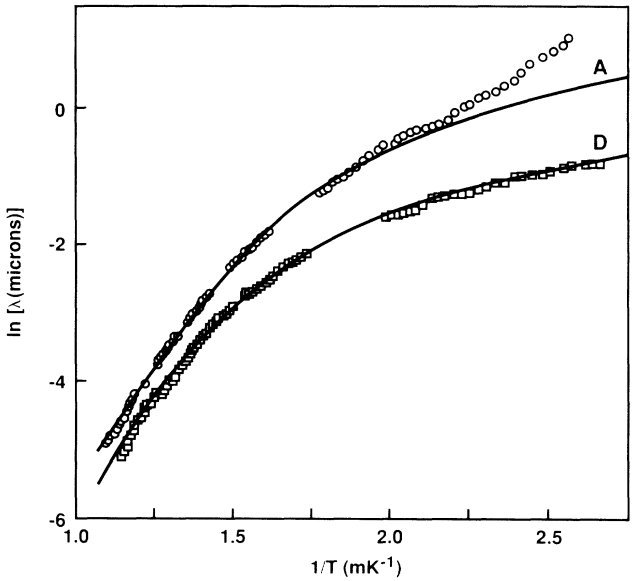

FIG. 4. The natural logarithm of the magnon mean free path λ as a function of inverse temperature (○, crystal A; □, crystal D). The activation energy determined from the high-temperature portion of each curve is estimated to be $5.8(\pm 0.3)$ mK. The solid lines through the data are fits as described in the text.

A, and 2.5 for crystal D. The reproducibility of our data is $\pm 10\%$, determined by melting crystals back to a 0.2-cm length and then regrowing them by taking data upon cooling as well as warming, and by reorienting the magnetic field. We observed only a 10%–20% decrease in the apparent mean free path when we tripled our magnetic field, owing to the smallness of the energy gap produced by the magnetic field and the absence of a spin-flop transition in this axially symmetric system.

For crystal A we find that $\lambda_0 = 1.17\times10^{-5}$ μm mK^2, $\lambda_1 = 7.22\times10^{-2}$ μm mK^3, and $\Delta/k_B = 5.8$ mK. For crystal D we find that $\lambda_0 = 7.43\times10^{-6}$ μm mK^2, $\lambda_1 = 3.83\times10^{-2}$ μm mK$^{2.5}$, and $\Delta/k_B = 5.8$ mK. These values of Δ are quite high compared to the calculated minimum energy for a zone-boundary magnon found in mean-field theory by Roger, Hetherington, and Delrieu[13] of 2.5 mK, probably reflecting the shortcomings of mean-field theory. While the second term in Eq. (2) fits the data quite well at low temperatures for crystal D, it fits only the intermediate-temperature data for crystal A, failing at very low temperatures where the mean free path rises almost exponentially below 0.5 mK with an activation energy of 2.7 mK. We have considerable confidence in these data, but have no explanation for what could be causing the mean free path to rise in this manner. We do note that for crystal A the heat flow is almost entirely along the ferromagnetic planes, and that, in this geometry, magnons would not be scattered by missing ferromagnetic planes as would result from dislocations in the crystal lattice. This might explain the difference in the exponent a for crystals A and D, but not the steep rise in λ at the lowest temperatures.

We wish to thank Daniel Fisher and Mike Cross for stimulating discussions and Ben Tigner for his technical assistance. We are grateful to AT&T Bell Laboratories for loaning to us the cryostat used in this experiment. This work has been supported by the NSF under Grant No. DMR-8803301.

[a]Present address: Department of Physics, Cornell University, Ithaca, NY 14853.

[1]C. Ni, H. N. Spector, and H. Weinstock, Phys. Rev. B **6**, 3370 (1972).

[2]R. L. Douglass, Phys. Rev. **129**, 1132 (1963).

[3]J. E. Rives, G. S. Dixon, and D. Walton, J. Appl. Phys. **40**, 1555 (1969).

[4]Vespel is manufactured by DuPont.

[5]D. D. Osheroff and R. C. Richardson, Phys. Rev. Lett. **54**, 1178 (1985).

[6]J. C. Wheatley, Rev. Mod. Phys. **47**, 415 (1975).

[7]T. Hata, S. Yamasaki, T. Kodama, and T. Shigi, J. Low Temp. Phys. **71**, 193 (1988).

[8]C. Kittel, *Introduction to Solid State Physics* (Wiley, New York, 1986), 5th ed.

[9]D. D. Osheroff, M. C. Cross, and D. S. Fisher, Phys. Rev. Lett. **44**, 792 (1980).

[10]D. S. Greywall, Phys. Rev. B **33**, 7520 (1986).

[11]D. D. Osheroff and C. Yu, Phys. Lett. **77A**, 458 (1980).

[12]D. S. Greywall and P. A. Busch, Phys. Rev. B **36**, 6853 (1987).

[13]M. Roger, J. H. Hetherington, and J. M. Delrieu, Rev. Mod. Phys. **55**, 1 (1983).

[14]J. Wilks, *The Properties of Liquid and Solid Helium* (Clarendon, Oxford, 1967).

[15]E. M. Lifshitz, and L. P. Pitaevskii, *Statistical Physics* (Pergamon, Oxford, 1986), Pt. 2.

[16]J. M. Ziman, *Electrons and Phonons* (Clarendon, Oxford, 1960).

[17]D. S. Fisher (private communication).